HIGH-PERFORMANCE TOMOGRAPHIC IMAGING AND APPLICATIONS

Hua Lee and Yuan-Fang Wang
Department of Electrical and Computer Engineering
University of California, Santa Barbara

ABSTRACT

Tomographic imaging systems utilize various probing waveforms, such as microwaves, acoustic and ultrasound, and light, for different application objectives. This paper provides a comprehensive overview of various tomographic imaging systems operating in different modalities of mono-static, bi-static, and multi-static format in both transmission and reflection modes. Tomographic acoustic microscopy, ground-penetrating radar imaging, synthetic-aperture sonar imaging, 3D medical endoscopy and terrain survey are included as direct examples of the imaging technology, with historical overview, physical modeling and system analysis, and experiments.

INTRODUCTION

Imaging represents the most direct and complete integration of sensing technology. Imaging functions in different modalities and applications. This paper provides a complete overview of a full range of imaging systems developed in the Imaging Systems Laboratory of the University of California, Santa Barbara. In this paper, the systems including tomographic acoustic microscopy, microwave subsurface imaging, synthetic-aperture sonar imaging, 3D medical endoscopy and terrain survey, are thoroughly described.

Conventional acoustic microscopy has been limited to the imaging of thin specimens. The research objective of tomographic acoustic microscopy is to achieve three-dimensional acoustic imaging at the microscopic scale and advance the resolving capability to the limit. The imaging modality is single-frequency transmission-mode with multiple illumination observation angles. The operating frequency of the illumination acoustic waves is 100 MHz, and the data acquisition of the acoustic wavefield is performed by a scanning laser beam. The direct applications are the 3D imaging of biological specimens and nondestructive evaluation.

One microwave subsurface imaging application is the ground-penetrating radar (GPR) imaging. Typically, it operates in the mono-static pulse-echo mode. Two-dimensional and three-dimensional survey is performed through synthetic aperture data acquisition. Applications include subsurface survey and NDE of civil structures.

Synthetic-aperture sonar imaging is the acoustic equivalent of SAR. It normally functions in the pulse-echo mode with a multi-element array. The applications cover a wide range of oceanic search. The use of a multi-element array is for the redundancy for the estimation and compensation of platform motion.

The concept of combining sub-images for system optimization can be applied to video-camera systems. 3D terrain survey and medical endoscopy are utilized to demonstrate the improvement and optimization of system performance in the optical domain.

In this paper, for each imaging application, the historical overview, system modeling and analysis, experiments, and field tests results will be presented.

MICROWAVE IMAGING

There are many applications of microwave imaging other than the conventional in-air radar imaging. One interesting and important application is the ground-penetrating radar (GPR) imaging. In terms of operating modality, it is a reflection-mode imaging within the microwave-frequency range. Typically, it operates in the mono-static pulse-echo mode. Two-dimensional or three-dimensional imaging can be achieved in the synthetic-aperture format. Important applications of GPR imaging are subsurface survey and nondestructive evaluation of civil structures.

The first experiment is performed with a GSSI GPR unit. The system consists of a bow-tie antenna as the transceiver. The illumination probing signal is a CW pulse at the operating frequency of 1 GHz, with an applicable bandwidth of approximately 100 MHz. For this experiment, it is operated in the mono-static pulse-echo mode with a planar two-dimensional synthetic aperture. The two-dimensional planar synthetic aperture was formed by repeating the linear scan. Then three-dimensional tomographic subsurface images can be reconstructed.

Figure (1) is the three-dimensional image of the internal structure of a concrete specimen, showing two layers of rebars. The image also shows the artifacts at the two corners, from the reflections from the edges of the specimen.
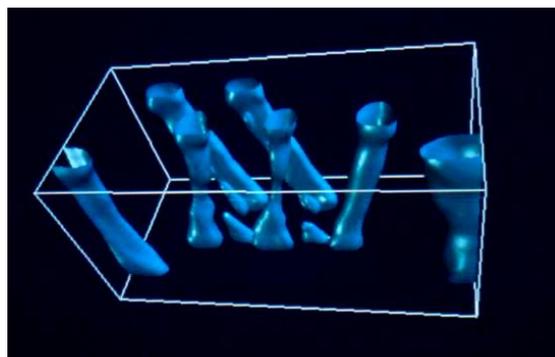

Figure (1): Three-dimensional image of the internal structure

As the technology advances, the operating modality changes accordingly. The second experiment is performed with a different GPR imaging system. This ground-penetrating radar is a fully software-defined unit. This system employs FMCW illumination waveforms, instead of the conventional use of a short time pulse as the probing waveforms. Vivaldi antennas are used as the transceivers for wideband high-gain operations.

The data set was taken over the walkway pavement. Figure (2-a) shows the walkway area during the repair process. After the repair, the GPR system scanned along a linear path and took data at *200* spatial positions. The spatial spacing between the data-collection positions is *0.0213 m (2.13 cm).* At each data-collection position, the system illuminates the walkway pavement with microwaves in the step-frequency mode, stepping through 128 frequencies, from *0.976 GHz* to *2.00 GHz*, with a constant increment. The relative permittivity for this experiment is set at 6.0.

Figure (2-a): Walkway area during the repair process

The image reconstruction algorithm can be implemented in two versions. One is to first form 128 holographic sub-images, corresponding to the 128 coherent wavelengths. The superposition of the 128 sub-images produces the final image. The second version first forms 200 range profiles at the 200 data-collection positions. The superposition of the range profiles produces the final images. These two versions give identical final images. Figure (2-b) shows the reconstructed image of subsurface rebar structure.
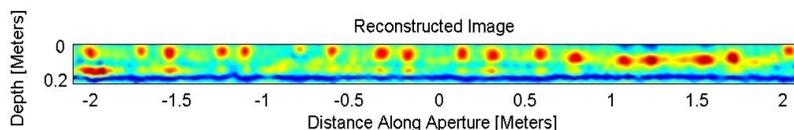

Figure (2-b): Image of subsurface rebar structure

ACOUSTICAL IMAGING

Synthetic-aperture sonar imaging is the acoustic equivalent of synthetic-aperture radar (SAR) imaging. Typical applications are oceanic search, survey, and underwater mapping.

It normally functions in the mono-static reflection mode. More recently, the functionality has been extended with multi-element transceiver array. The use of multi-element arrays is to provide the redundancy to enable the estimation of platform motion which is common in practical deployment. There exist six parameters in 3D motion estimation, of which three are associated with the translational-motion vector and the other three are associated with the rotation matrix in three dimensions.

The field experiment was conducted in the San Diego Bay with a linear 10-element sonar array operating in the side-looking linear-scan model. The synthetic aperture in one-dimensional and the objective of the imaging experiment is the two-dimensional planar ocean floor. Figure (3) is the reconstructed image of a sunken airplane.

Figure (3): Sonar image of a sunken airplane

Acoustical imaging can function in both transmission and reflection mode. The scanning tomographic acoustic microscopy (STAM) is an excellent example of acoustical imaging operating in the transmission mode. Its exact imaging modality is classified as single-frequency illumination in the transmission mode with multiple observation angles. The operating frequency of the illumination acoustic plane waves is 100 MHz, and the data acquisition of the acoustic wavefield is performed by a focused laser beam scanning over a 2D aperture, followed by a knife-edge detector.

Subsequent to the knife-edge detector, the detected signal is down-converted from 100 MHz to 32.4 MHz. Then a quadrature receiver, operating at 32.4 MHz, estimates both the amplitude and phase of the waveforms. The full complex waveforms over the two-dimensional aperture are then backward propagated down toward the 3D subsurface region to form a holographic image.

Figure (4) shows a STAM image of a subsurface test specimen to demonstrate the capability of holographic acoustical imaging at microscopic scale.
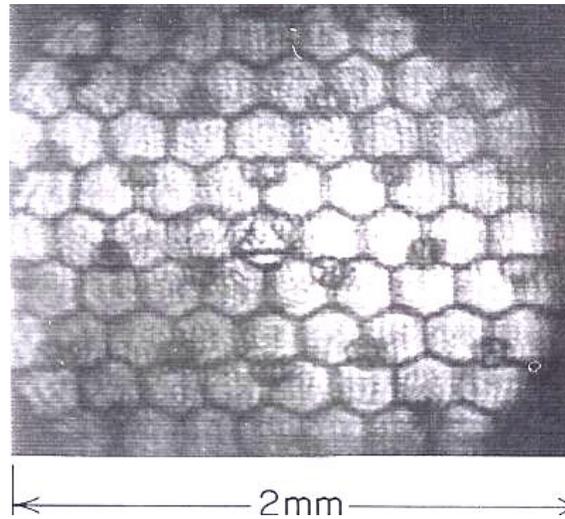

Figure (4): STAM image of a subsurface test specimen

Corresponding to each coherent wavelength, a holographic image of the specimen can be reconstructed. To improve the range resolution, a rotation stage is added to the data-acquisition device to extend the system to the level of multi-angle tomography. A two-layer specimen is used to test the resolving capability in the depth direction. Figure (5-a) is STAM image of the first layer, and Figure (5-b) shows image of the second layer.
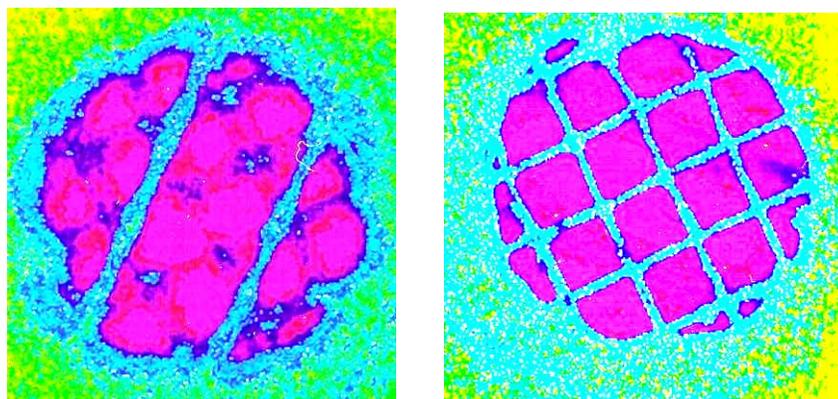

Figure (5-a): STAM image of the first layer; Figure (5-b): image of the second layer

THREE-DIMENSIONAL MEDICAL ENDOSCOPY AND TERRAIN SURVEY

In acoustic and microwave imaging, the resolving capability of the systems is governed by the coverage and bandwidth of the spatial-frequency spectrum, which involves the size of the receiving aperture, angle of the active illumination, and bandwidth of the probing waveforms. To improve system performance, the typical approach has been the expansion of aperture size, observation angular coverage, and probing signal bandwidth, to elevate the systems to the level of multi-frequency or multi-projection tomography.

In the optical domain, the system optimization is achieved through the expansion of the observation perspective. The procedure is to first integrate the sub-images from various perspective angles to construct the 3D image profile. The superposition produces the variation in the depth direction and improves the resolution through background noise reduction. Subsequently, the user can view the 3D profile from any selected perspective. Conceptually, this has a high degree of equivalence to multi-projection tomography in acoustical and microwave imaging.

One interesting application of this approach is 3D medical endoscopy. Figure (6-a) shows the procedure of combining 2D image frames for the estimation of the 3D profile. After the formation of the 3D profile, it can be viewed from any elected perspective, which is of critical importance to the precision in the surgical procedures. Figure (6-b) shows the view of the 3D profile from six different perspective angles. This capability allows the surgeons to examine the region of interest from the preferred perspective to improve the effectiveness of hand-eye coordination in a dynamic manner.
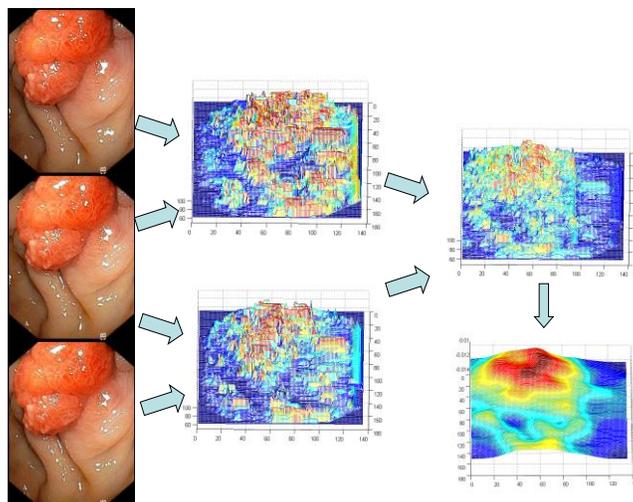

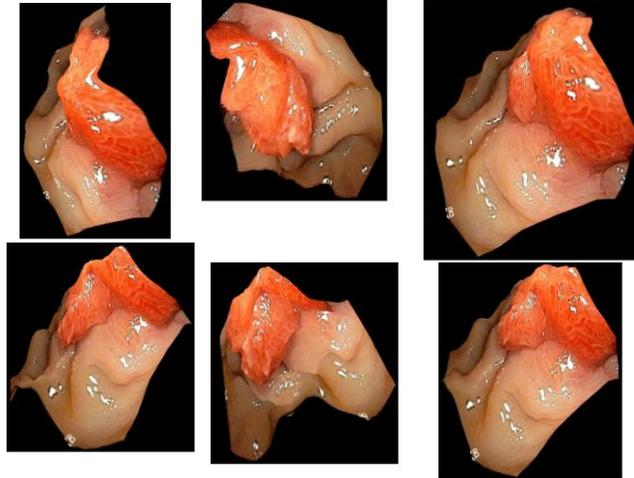Figure (6-a): Combination of 2D image frames for the estimation of the 3D

Figure (6-b): Views from six different perspective angles

Similarly, the concept can be applied to the topographic survey of 3D terrains. Figure (7-a) shows the 3D composite image from the video sequence recorded during the survey flight. The circular flight path is marked in red in the photo. The algorithm also provides the estimates of the data-acquisition positions, as part of the process.
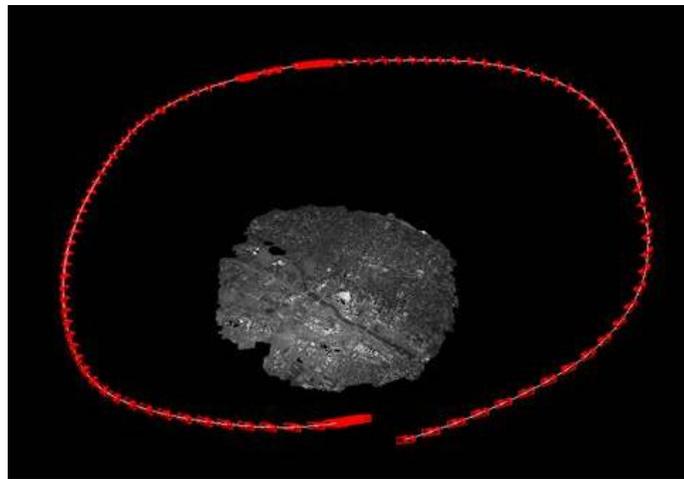

Figure (7-a): 3D composite image from a survey flight

By combining the 2D image frames accurately from the video sequence, a 3D terrain profile can be constructed and stored. Then it can be viewed from any selected perspective. Figure (7-b) is the enlarged version of the 3D reconstructed profile, viewed from a selected view angle.
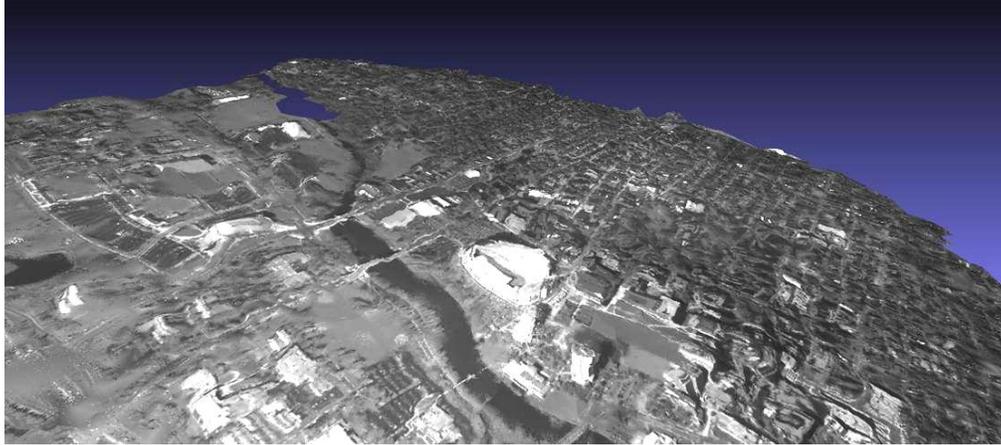
Figure (7-b): Enlarged version of the 3D reconstructed profile

CONCLUSION

This paper provides an overview of tomographic acoustic microscopy, ground-penetrating radar imaging, synthetic-aperture sonar imaging, 3D medical endoscopy and terrain survey, as examples of the design, development, system integration and optimization of tomographic imaging systems. The purpose is to compare system functions and applications with various probing signals, operating modalities, and system configurations. Laboratory and field experiments were included to demonstrate the effectiveness of the system performance.

REFERENCES

1. Hua Lee and Glen Wade, *Imaging Technology*, IEEE Press, New York, 1986.
2. Zse-Cherng Lin, Hua Lee, and Glen Wade, "Scanning Tomographic Acoustic Microscope: A Review," *IEEE Transactions on Sonics and Ultrasonics*, vol. SU-32, no. 2, pp. 168-180, March 1985.
3. Hua Lee and Carlos Ricci, "Modification of the Scanning Laser Acoustic Microscope for Holographic and Tomographic Imaging," *Applied Physics Letters*, 49(20), pp. 1336-1338, November 1986.
4. Zse-Cherng Lin, Hua Lee, Glen Wade, Michael G. Oravecz, and Lawrence W. Kessler, "Holographic Image Reconstruction in Scanning Laser Acoustic Microscopy," *IEEE Transactions on Ultrasonics, Ferroelectrics, and Frequency Control,* vol. UFFC-34, no. 3, pp. 293-300, May 1987.
5. Richard Y. Chiao and Hua Lee, "Scanning Tomographic Acoustic Microscopy," *IEEE Transactions on Image Processing,* 4(3), pp. 358-369, March 1995.
6. Brett L. Douglas, John M. Silkaitis, and Hua Lee, "Single-Reference Calibration Technique for Multiple-Element Array Sonar Imaging Systems," *Journal of Acoustical Society of America,* 100(1), pp. 400-407, July 1996.

7. Bretton L. Douglas and Hua Lee, "Synthetic-Aperture Sonar Imaging with a Multiple Element Receiver Array," *Proceedings of IEEE International Conference on Acoustics, Speech and Signal Processing,* pp. V 445-448, 1993.
8. John M. Silkaitis, Brett L. Douglas, and Hua Lee, "Motion Compensation in Synthetic Aperture Sonar Imaging," *Acoustical Imaging*, Vol. 21, Joie P. Jones Ed., Plenum Press, pp. 745-754, 1995.
9. Hua Lee, "Motion Compensation by Phase Correction for Synthetic-Aperture Side-Scan Sonar Imaging," *International Journal on Imaging Systems and Technology,* Vol. 14, pp. 159-261, 2005.
10. Michael S. D'Errico, Bretton L. Douglas, and Hua Lee, "Subsurface Microwave Imaging for Nondestructive Evaluation of Civil Structures," *Proceedings of IEEE International Conference on Acoustics, Speech and Signal Processing,* pp. V 453-456, 1993.
11. Hua Lee and Joseph P. Murtha, "Pulse-Echo Microwave Tomographic Imaging and Object Recognition for NDE of Civil Structures and Materials," *Proceedings of the Second International Conference on Imaging Technologies: Techniques and Civil Engineering Applications,* 1997.
12. H. Lee, "An Overview of Synthetic-Aperture Image Reconstruction Algorithms for GPR Imaging with Pulse-Echo and Step-Frequency FMCW Systems," *Journal of Environmental and Engineering Geophysics,* 8(2), pp. 105-114, June 2003.
13. D. Koppel, Y.F. Wang, and H. Lee, "Automated Image Rectification in Video-Endoscopy," *Proceedings of the 4th International Conference on Medical Image Computing and Computer-Assisted Intervention,* 2001.
14. D. Koppel, Y. Wang, and H. Lee, "Image-Based Rendering and Modeling in Video-Endoscopy," *Proceedings of the IEEE International Symposium on Biomedical Imaging*, 2004.
15. Dan Koppel, Yuan-Fang Wang, and Hua Lee, "Image-Based View Rendering in Endoscopy," *International Journal on Imaging Systems and Technology*, Vol. 14, pp. 181-185, 2005.